Creating novel fungicides by targeting Cdc14 in *Fusarium oxysporum*

Xi Chen and Ecem Sena Uluegeci
Advisors: Mark C. Hall (Purdue University), Martha Oakley (Indiana University Bloomington)
Summer Science Program in Biochemistry 2018, Purdue University

---

ABSTRACT

Widespread fungal pathogen attacks in recent years have compromised important crops, making it more important than ever to produce efficient fungicides. In confronting this current issue, our research team focused on the inhibition of Cdc14, a dual-specificity phosphatase with an important role in regulating exit from mitosis. Previous research demonstrates its importance in the mitotic exit network (MEN) and for cell development; mutations and removal of Cdc14 in fungal species resulted in inhibition of pathogenicity. Due to its absence in plant species but conservation and importance in fungal species, Cdc14 is an ideal target for fungal inhibition. To better understand Cdc14 in fungal strains such as *Fusarium oxysporum*, a pathogen that has caused widespread crop disease, we performed substrate specificity assays to analyze the active site of *Fusarium oxysporum* Cdc14 (FoCdc14) as the target location for an inhibitor. We then characterized the enzyme kinetics using Michaelis-Menten analysis and assays. The kinetics and mechanism of inhibition of potential inhibitors were also determined using assays. Our data shows two potential inhibitors for further development, labeled in our experiment as I1 and I2, which are competitive and uncompetitive inhibitors respectively. Due to the favorability of a competitive inhibitor, we focused on I1 and used modeling equipment such as the Molecular Operating Environment (MOE) to optimize binding affinity of inhibitor I1 to FoCdc14. Our results reveal a chemical capable of inhibiting Cdc14 in fungal species and aiding the global pandemic of fungal pathogen attacks.

Keywords: Cdc14, phosphatase, dual-specificity phosphatase, Michaelis-Menten kinetics, fungicide, mitosis

With the world's population expected to exceed 10 billion by the turn of the century[1], it is more important than ever to increase production of healthy crops. Complications in global food security, world hunger, climate change, and decreased availability of land already make sufficient crop production more difficult than it has been in past decades. Furthermore, a growing number of plant pathogen attacks by fungi has wreaked havoc on important crops. With relatively few and mostly ineffective fungicides doing little as preventive measures, species such as *Fusarium oxysporum*, responsible for wiping out an entire species of banana in the 20th century[2], are infesting and deteriorating important crops.

Thus, in the search for a highly effective, commercially viable new fungicide, our research team has focused on the protein Cdc14. First characterized in 1974 by Leland H. Hartwell et al., this family member of dual-specificity phosphatases regulates mitosis in *Saccharomyces cerevisiae*[3]; further studies showed that it controlled mitotic exit by reversing phosphorylation by cyclin-dependent kinase 1 (Cdk1) in yeast[4]. Removal of the Cdc14 sequence interferes with the Mitotic Exit Network (MEN), a signaling pathway that promotes mitotic exit and initiates cytokinesis[4][5][6][7]. Cdc14 is a vital part of the network; mutants lacking the phosphatase freeze in telophase and are unable to continue cell division, inhibiting fungal pathogenicity[7][8]. Outside of *S. cerevisiae*, Cdc14 has been found to have alternate, but still essential, tasks, such as entering mitosis and regulating spindle orientation in *Saccharomyces pombe* (fission yeast) and localizing spindles in metazoa[9][10]. Thus, failure of Cdc14 will inhibit pathogenicity in a variety of organisms. This is one of three major reasons why a fungicide targeting it would be a highly marketable product - its efficiency and degree of success would be unparalleled.

Furthermore, Cdc14 is a highly conserved gene[10]. It can be found in most eukaryotes and fungal species. This, of course, drives an important question: is it too conserved? A fungicide targeting such an area will affect a broad range of pathogens, yes, but it will also affect a broad range of other species - namely, the very crops that we are trying to save. Fortunately, Cdc14 is not found in plants[11]. It is very likely that the essential role of this phosphatase is simply not necessary in plants due to different mechanisms of cell division[12]. The conservation of Cdc14 means that an inhibitor targeting it will affect many fungal species, making it a highly marketable product. Cdc14's conservation among pathogen species, coupled with its nonexistence in plant species, make it an attractive potential target for new fungicides.

Finally, previous research on Cdc14 and related phosphatases show a unique active site that led us to our idea for an inhibitor fungicide[13][14]. We can see how substrates are recognized by Cdc14 by looking at co-crystal structures of Cdc14 bound to substrates. Biochemically, Cdc14 has a strict specificity for certain substrates. By mimicking these motifs, we can achieve a very specific inhibition of Cdc14 without affecting other enzymes. This is an important factor to take into account, as an inhibitor that binds to other proteins could lead to adverse effects in our crops.

Cdc14's importance, conservation, and specificity make it a viable target for the production of an artificial inhibitor that will benefit both industry and farmers. Through experimental procedures including enzyme assays and protein modeling using programs such as the Molecular Operating Environment (MOE), we have discovered and tested such an inhibitor as a possible product.

RESULTS AND DISCUSSION

Preparation of FoCdc14 for kinetics characterization.

Multisequence alignment of putative ortholog gene from *Fusarium oxysporum* across the known Cdc14 genes of diverse species including *Schizosaccharomyces pombe, Saccharomyces cerevisiae, Caenorhabditis elegans, Drosophila melanogaster, Homo sapiens*, and our target fungus, *Fusarium oxysporum*, found extensive conservation in regions known to be crucial for Cdc14 activity and function (Fig.1). Most notable was an area of 12 conserved residues (Fig.1 Residues 342-352, highlighted in yellow), known to be the active site and thus strongly suggesting that the gene is a Cdc14 ortholog in *F. oxysporum*.

To better characterize the *Fusarium oxysporum* Cdc14 ortholog (FoCdc14), we overexpressed the protein in plasmid pET15b from *E. coli* cells with a 6xHis tag and purified it using nickel affinity chromatography from a soluble cell extract. Induction of FoCdc14 in *E. coli* cells from plasmid pET15b was confirmed using gel electrophoresis (Fig.2A). The thicker band at 54 kDa in the induced column confirmed that the protein had been successfully made. Gel electrophoresis was also used to confirm the purification of FoCdc14 (Fig.2B). Following purification by nickel affinity chromatography from soluble cell extracts, comparison of the extract (pre-purification solution) and flowthrough from protein purification demonstrates removal of FoCdc14 from other proteins and cell debris. The purified protein displays a single band at around 54 kDa with no contaminants present.

An enzyme assay using the generic phosphatase substrate pNPP with and without orthovanadate inhibition was performed to confirm that the purified protein exhibited Cdc14-like phosphatase activity (Fig.2C). Averaged from three trials, the specific activity of FoCdc14 without inhibitor was about 3.3 μM/min with a standard deviation of 0.2. The specific activity of FoCdc14 with inhibition by orthovanadate was about 0.7 μM/min with a standard deviation of 0.1. There was a clear difference between the specific activity of the enzyme with and without the presence of orthovanadate, which structurally mimics phosphates and is a good inhibitor of all tyrosine phosphatase family members, including Cdc14. Thus, its ability to inhibit our purified protein suggests that it is indeed a Cdc14 ortholog. The concentration of purified protein was then determined through Bradford assay to be 160 μM.

Using the Molecular Operating Environment (MOE), we created a homology model for FoCdc14 based on the yeast Cdc14 (Fig.2D) complex. The resulting structure was used for docking and optimization later on in the study.

FoCdc14 Michaelis-Menten kinetics characterized by assay.

An assay measuring rate of pNPP dephosphorylation as a function of pNPP concentration under steady-state conditions was run in triplicate to characterize the Michaelis-Menten kinetics of FoCdc14 and determine its k_{cat} and K_m. The average k_{cat} was 0.4 s^{-1} with a standard deviation of 0.1 and the average K_m was 40 mM with a standard deviation of 7.3, determined from three trials (Fig.3). The information from this graph helped characterize FoCdc14 as a dual-specificity phosphatase, as the K_m value

corresponds to reported K_m values for Cdc14 orthologs. The K_m value was later used to set up conditions for inhibitor screening assays.

FoCdc14 exhibits similar substrate specificity to yeast Cdc14.

An assay measuring dephosphorylation of each substrate was run in triplicate to determine the catalytic efficiency (k_{cat}/K_m) of 24 different substrates (Table 1) and better characterize FoCdc14 (Fig.4). We hypothesized that the best substrates would have a phosphoserine, basic residues on the +3, +4, and +5 positions, and a proline on the +1 position based on previous research[15] and a multisequence alignment. We used the catalytic efficiency (k_{cat}/K_m) of each substrate to rank them (Fig.4). There was a strong correlation between the substrates that we predicted to have high affinity for FoCdc14 and the ones that actually did, helping us grasp a better idea of how to optimize an inhibitor to fit into the active site. We found that the presence of a phosphoserine was especially important for recognition. Presence of all three criteria gave the highest catalytic efficiency.

Inhibitor screening assay.

To predict how a collection of candidate inhibitors identified for yeast Cdc14 might bind to the active site of FoCdc14, we retrieved and compared the docking score and empirical data through the Molecular Operating Environment (MOE) and wet lab techniques (see Table 2B and Fig.5). Using MOE, we simulated the docking of the inhibitor in the active site of FoCdc14. Scores for docking ranged from -4 to -6 kcal/mol. We then performed an assay with pNPP to compare the inhibitors using a constant substrate concentration determined by the K_m from above. Percent inhibition ranged from 30% to over 100%. The most effective inhibitors were mainly determined from the empirical assay results, although Docking Score was taken into account. Inhibitors I1 and I2 were chosen as two of our best inhibitors, due to their high docking scores as well as percent inhibition. Despite its low docking score, we additionally decided to test inhibitor H5 since it showed promise in the empirical trials.

Using an IC_{50} assay, the IC_{50} values of our top three inhibitors were then measured so we could select one molecule to move forward with optimization and characterization (Fig.6). We received a very low IC_{50} of 9.8 μM for inhibitor I1. Inhibitor I2 yielded a relatively higher IC_{50} of 34.4 μM, while inhibitor H5 yielded a very high IC_{50} of 217.5 μM. A lower IC_{50} is ideal, as it will take less of the inhibitor to inhibit FoCdc14. This assay determined our best inhibitor as I1, with I2 following close behind. This correlated with the results of our inhibitor screening. Our research team decided to characterize the method of inhibition of I2, while our collaborators, also working on FoCdc14, continued with I1.

Characterizing mechanism of inhibition.

Two assays were used to characterize the mechanism of inhibition of our top inhibitor, I2. An assay to determine the reversibility of the inhibitor was run and determined that I2 bound reversibly to the enzyme due to lack of correlation between pre-incubation time and inhibition (Fig.7A). It was interesting to note how low the absorbance of the 0 minute pre-incubation tubes were in comparison to the others; we recommend further study with longer pre-incubation times in the future. A Michaelis-Menten enzyme assay was then performed to pinpoint the specific mechanism of inhibition (Fig.7B). In testing inhibitor

I2, we found that its k_{cat} and K_m both decreased as the concentration of inhibitor increased (a k_{cat} of 23.35, 12.64, and 5.29, and a K_m of 62.11, 28.16, and 13.21 for inhibitor concentrations of 0 μM, 25 μM, and 50 μM, respectively), a characteristic of uncompetitive inhibitors. While uncompetitive inhibition is not the most favorable method, as we cannot determine its specificity to the Cdc14 phosphatase alone, we would recommend further study on the specific interactions between this inhibitor and FoCdc14 to classify it as a potential fungicide. In moving forward with the project, we used an inhibitor that had both scored high during inhibitor screening and was found to be competitive by collaborators also working on *Fusarium oxysporum*, I1.

Optimization of inhibitor I1.

The inhibitor I1 originally had an affinity of -7.74 kcal/mol (Fig. 8A) after docking and energy minimization for our homology model of FoCdc14. Following optimization to make I1 better fill the active site and interact with the receptor, we improved the affinity to -14.20 kcal/mol (Fig. 8B). Affinity to the active site was improved by using a carbon backbone and benzene rings to better shape the inhibitor (Fig. 8C). Additionally, a phosphonate group was added to a back pocket, mimicking a natural substrate of FoCdc14 without the issue of being hydrolyzed by the enzyme.

EXPERIMENTAL PROCEDURES

Bacterial Transformation

The *Fusarium oxysporum* Cdc14 protein (FoCdc14) was transformed into bacterial *E. coli* BL21AI cells in 450 uL 2xYT medium (5g NaCl, 16g tryptone, 10g yeast extract, 1L H_2O). 50 uL of each tube was then aliquoted to a corresponding LB-ampicillin plate. The plates were then incubated at 37°C overnight.

Protein Purification

Following set-up of an Akta Protein Purification System, a soluble extract from *E. coli* was prepared for nickel purification using a nickel column, 250 mL Nickel Buffer A (25 mM HEPES pH 7.5, 500 mM NaCl, and 10% glycerol in H_2O), and 250 mL Nickel Buffer B (25 mM HEPES pH 7.5, 500 mM NaCl, 250 mM imidazole, and 10% glycerol in H_2O). 12 tubes of the purified protein were saved after analysis of the protein purification graph. The collected protein was then further purified through overnight dialysis in 1L storage buffer (25 mM HEPES pH 7.5, 300 mM NaCl, 2 mM EDTA, 0.1% 2-mercaptoethanol, and 40% glycerol in H_2O) and transferred into 250 uL aliquots. Using this resulting solution, we used a Bradford assay to determine the concentration of our protein. We also confirmed our protein identity using Protein Mass Fingerprinting.

Running Gels to Test Uninduced/Induced and to Confirm Purification

SDS-PAGE gels composed of resolving gel (8.2 mL H_2O, 5 mL resolving gel buffer [1.5 M tris-HCl], 6.5 mL 30% acrylamide:bis-acrylamide solution, 200 uL 10% SDS, ammonium persulfate [APS], and TEMED) and stacking gel (2.5 mL stacking gel buffer [0.5 M tris-HCl], 6.4 mL H_2O, 100 uL 10% SDS, 1 mL 30% acrylamide/bis-acrylamide solution, 50 uL 10 APS, and 10 uL TEMED) were run in running buffer at a constant voltage of 180 for one hour to confirm protein purification. These gels were then used to test induction of protein (by running molecular markers, a sample of induced protein, and a sample of uninduced protein) and purification of protein (by running molecular markers, an extract of unpurified protein, a sample of flowthrough, the purified protein, and a protein of known molecular weight).

Activity Assay

Two tubes containing 400 uL of reaction buffer (25 mM Hepes, 1.1% 2-mercaptoethanol, 1 mM EDTA, and 150 mM NaCl in 200 mL H_2O)), 0.1 μM enzyme, 40 mM substrate (para-nitrophenyl phosphate [pNPP]), and either 50 mM sodium orthovanadate or 0 mM sodium orthovanadate were incubated at 30°C for 20 minutes. 100 uL 5N NaOH was used to stop each reaction. Each tube was measured at a wavelength of 405.4 nm in a spectrophotometer. The specific activity of the enzyme was calculated using the measured absorbance using the following equation.

$$absorbance = \xi \cdot c \cdot l$$

Homology Modeling with MOE

The target sequence of FoCdc14 and the Cdc14 structure from yeast (5XW5) were used to generate a homology model in the Molecular Operating Environment (MOE).

Characterization of FoCdc14 by Enzyme Assays

Unless otherwise noted, all subsequent enzyme assays were run in 100 uL of enzyme reaction buffer (25 mM Hepes, 1.1% 2-mercaptoethanol, 1 mM EDTA, and 150 mM NaCl in 200 mL H_2O) for 20 minutes at 30°C (steady-state, determined using previous research) before being stopped with 25 uL of 5N NaOH. Absorbances were read in a 96-well microplate at 405 nm. Appropriate blanks were run to account for background noise such as inherent absorbance of the substrate and inhibitors.

Michaelis-Menten Assay

An enzyme assay to generate a Michaelis-Menten curve was performed using 80 mM, 60 mM, 40 mM, 20 mM, 10 mM, 5 mM, 2 mM, and 0 mM para-nitrophenyl phosphate (pNPP) and 0.2 μM enzyme. The resulting absorbances were then converted to velocity (v_0) and graphed against the concentration of substrate ([pNPP]). Using the Michaelis-Menten curve equation ($\frac{Ax}{B+x}$), a k_{cat} and K_m value were calculated for use in the next assays.

Substrate Selectivity Assay

The assay was run in triplicate with 24 substrates (Table 1) of varied theoretical affinities at a final concentration of 100 μM and enzyme at a final concentration of 0.1 μM in 50 uL for 20 minutes at 30°C. 100 uL Biomol green dye was used to stop the reaction. Following 20 minutes of incubation with Biomol green at room temperature, the tubes were read in a microplate spectrophotometer at 640 nm.

Inhibitor Docking

Using the previously generated homology model, 16 structures of different inhibitors were modeled and docked to an active site *in silico*. The best scores or positions were noted to make comparisons between inhibitors (Fig.5A).

Inhibitor Screening Assay

Preceding the trials, a z-factor trial was performed to determine the reliability of our assays in assessing inhibitor activity. Trials were performed with 1 μM enzyme, 500 μM inhibitor (or 2 mM for inhibitors H5, H6, and H7 from the Fraction Library). Two control tubes were run to measure 100% (enzyme and substrate) vs. 0% activity (substrate only). Our substrate was pNPP at the concentration of 30 mM. These reactions were run at 30°C for 20 minutes.

IC_{50} Assay

An IC_{50} curve was determined for three of our top inhibitors, I1, I2, and H5. Dilutions of the inhibitors were added to the experimental tubes to achieve starting final concentrations of 500 μM for inhibitors I1 and I2 and 2000 μM for inhibitor H5.This assay also included two controls: one without enzyme and inhibitor, one without enzyme. Two-fold serial dilutions were made from this point (i.e. 500, 250, 125, 62.5, 31.25, 15.625, 7.8125, 3.91, 1.95, 0.98 μM inhibitor I1) until we would have 10 data points to work with on our curve. The tubes also contained 30 mM substrate (pNPP) and 1 μM enzyme. These reactions were run at 30°C for 20 minutes and stopped with 25 uL of 5N NaOH.

Mechanism of Inhibition

An assay was run in triplicate to determine if the inhibitor I2 was reversible or irreversible. The trial was performed with 1 μM enzyme, 30 mM pNPP, and 300 μM inhibitor. The enzyme-inhibitor-buffer solution

was allowed to sit for four different pre-incubation times (0, 15, 30, and 60 minutes) before beginning the reaction with substrate. The method of inhibition of I2 was determined through Michaelis-Menten kinetics. Three different concentrations of inhibitor were tested: 0, 25, and 50 μM (slightly below and above the IC_{50} value). For each concentration of inhibitor, eight concentrations of pNPP (80, 60, 40, 20, 10, 5, 2, and 0 mM) were tested. Each tube contained reaction buffer, inhibitor, substrate, and 1 μM of enzyme. Each reaction was run at 30°C for 20 minutes. They were stopped with 25 uL of NaOH dilution.

Computational Optimization

Using the previously generated homology model, the chosen inhibitor (I1) was redocked into the active site. More molecules (including oxygens, benzene rings, nitrogen, a phosphorus) were added to increase affinity for the active site in order to create a molecule with the highest potential as a fungicide. The molecules added were dependent on the characteristics of the active site (acidity, hydrophilicity, etc.).

References

1. United Nations, Department of Economic and Social Affairs, Population Division (2017). World Population Prospects: The 2017 Revision, Volume I: Comprehensive Tables. T/ESA/SER.A/399.
2. Zheng, S. J., Gracia-Bastidas, F. A., Li, X., Zeng, L., Bai, T., Xu, S., Yin, K., Li, H., Fu, G., Yu, Y., Yang, L., Nguyen, H. C., Douangboupha, B., Khaing, A. A., Drenth, A., Seidl, M. F., Meijer, H. J. G., & Kema, G. H. J. (2018). New geographical insights of the latest expansion of *Fusarium oxysporum* f. sp. *cubense* tropical race 4 into the greater Mekong subregion. *Frontiers in Plant Science.* https://doi.org/10.3389/fpls.2018.00457
3. Hartwell, L. H., Culotti, J., Pringle, J. R., & Reid, B. J. (1974). Genetic control of the cell division cycle in yeast. *Science, 183,* 46-51. http://doi.org/10.1126/science.183.4120.46
4. Powers, B. L., & Hall, M. C. (2017). Re-examining the role of Cdc14 phosphatase in reversal of Cdk phosphorylation during mitotic exit. *Journal of Cell Science, 130,* 2673-2681. http://doi.org/10.1242/jcs.201012
5. Li, C. H., Melesse, M., Zhang, S. J., Hao, C. F., Wang, C. F., Zhang, H. C., Hall, M. C., & Xu, J. R. (2015). FgCdc14 regulates cytokinesis, morphogenesis, and pathogenesis in *Fusarium graminearum*. *Molecular Microbiology, 98*, 770-786. http://doi.org/10.1111/mmi.13157
6. Nasa, I., & Kettenbach, A. N. (2018). Coordination of Protein Kinase and Phosphoprotein Phosphatase Activities in Mitosis. *Frontiers in Cellular and Infection Microbiology, 6*, 30. http://doi.org/10.3389/fcell.2018.00030
7. Baro, B., Queralt, E., & Monje-Casas, F. (2016). Regulation of mitotic exit in *Saccharomyces cerevisiae. Methods in Molecular Biology, 1505*. https://doi.org/10.1007/978-1-4939-6502-1_1
8. Zhang, Z. Y. (2008). Protein-Tyrosine Phosphatases: Biological Function, Structural Characteristics, and Mechanism of Catalysis. *Critical Reviews in Biochemistry and Molecular Biology, 33,* 1-52. https://doi.org/10.1080/10409239891204161
9. Mocciaro, A., & Schiebel, E. (2010). Cdc14: a highly conserved family of phosphatases with non-conserved functions? *Journal of Cell Science, 123,* 2867-2876. http://doi.org/10.1242/jcs.074815
10. Yang, G., & Hu, Y., & Fasoyin, O. E., & Yue, Y., & Chen, L., & Qiu, Y., & Wang, X., & Zhuang, Z., & Wang, S. (2018). The Aspergillus flavus Phosphatase CDC14 Regulates Development, Aflatoxin Biosynthesis and Pathogenicity. *Frontiers in Cellular and Infection Microbiology, 8,* 141. doi: http://doi.org/10.3389/fcimb.2018.00141
11. Moorhead, G. B. G., De Wever, V., Templeton, G., & Kerk, D. (2008). Evolution of protein phosphatases in plants and animals. *Biochemical Journal, 417,* 401-409. http://doi.org/10.1042/BJ20081986
12. Inze, D. (2003). Why should we study the plant cell cycle? *Journal of Experimental Botany, 54*, 1125-1126. https://doi.org/10.1093/jxb/erg138
13. Wang, W. Q., & Bembenek, J., & Gee, K. R., & Yu, H., & Charbonneau, H., & Zhang, Z. Y. (2004). Kinetic and mechanistic studies of a cell cycle protein phosphatase Cdc14. *Journal of Biological Chemistry*. http://doi.org/10.1074/jbc.M402217200
14. Kobayashi, J., & Matsuura, Y. (2017). Structure and dimerization of the catalytic domain of the protein phosphatase Cdc14p, a key regulator of mitotic exit in Saccharomyces cerevisiae. *Protein Science, 10,* 2105-2112. http://doi.org/10.1002/pro.3244

15. Li, C., Melesse, M., Zhang, S., Hao, C., Wang, C., Zhang, H., Hall, M. C. and Xu, J. (2015). Functions of Cdc14 in Fusarium graminearum. *Molecular Microbiology, 98*, 770-786. http://doi.org/10.1111/mmi.13157

Acknowledgements: The authors would like to acknowledge Zachary Lee, Sydney Tsuyuki, and Cameron Uy for their help in characterizing FoCdc14 and inhibitors. The authors would also like to acknowledge Dr. Mark Hall, Dr. Martha Oakley, Hannah Nikole Almonte, Jacob Crosser, Emily Overway, Devin Srivastava, and John Whitney for their help with the study. The authors would finally like to acknowledge the 35 participants of the 2018 Purdue Biochemistry Summer Science Program for their unending support.

Conflict of interest: The authors declare that they have no conflicts of interest with the contents of this article.

APPENDIX

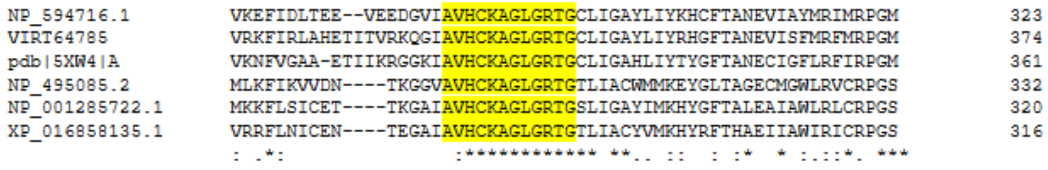

Figure 1. Conservation of FoCdc14 across species. FoCdc14 (Virt64785) was compared to sequences (found through BLAST Search) of *Schizosaccharomyces pombe* (NP_594716.1), *Saccharomyces cerevisiae* (pdb|5XW4|A), *Caenorhabditis elegans* (NP_495085.2), *Drosophila melanogaster* (NP_001285722.1), and *Homo sapiens* (XP_016858135.1). The most highly conserved region, hypothesized to be the active site, is highlighted in yellow. Asterisks indicate parts of the sequence conserved across all sequenced species.

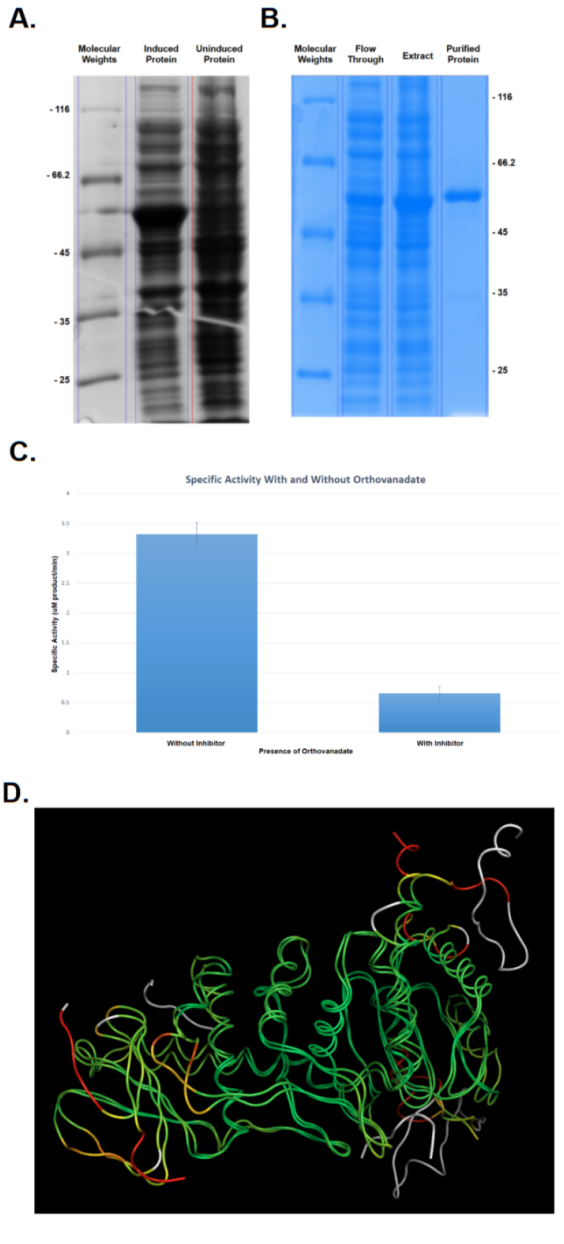

Figure 2. Preparation of FoCdc14 for characterization studies. (A) A sample with L-arabinose induced FoCdc14 is compared with a sample of uninduced protein. (B) The flowthrough from protein purification is compared to an extract of the unpurified solution and purified FoCdc14. (C) The specific activity in μM product/min. for 10 μM enzyme was measured in triplicate. The results with orthovanadate and without orthovanadate demonstrate that FoCdc14 has phosphatase activity. (D) A homology model based on the sequence of FoCdc14 and yeast Cdc14 was created in the Molecular Operating Environment (MOE). The homology model is shown here superposed against the yeast Cdc14 model (5XW5). The areas of highest similarity are shown in green while unrelated regions are shown in red.

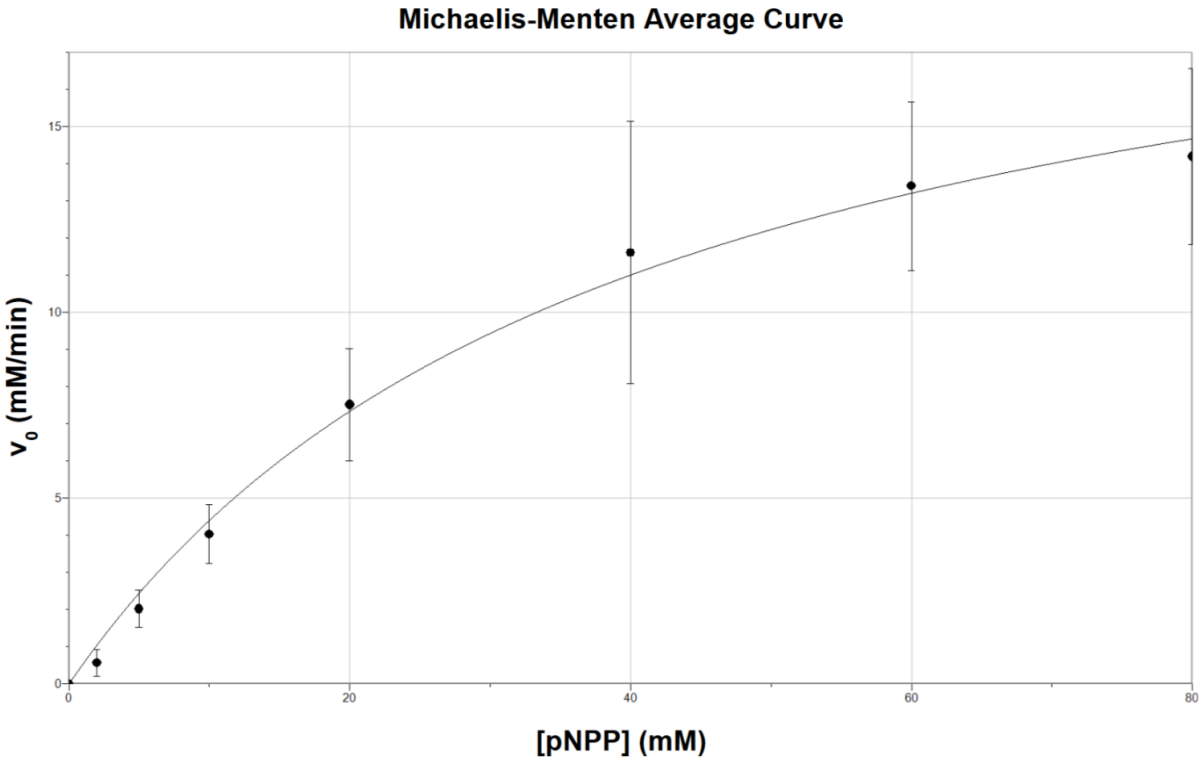

Figure 3. Characterization of kinetics of FoCdc14. The concentration of substrate ([pNPP]) was graphed against the initial velocity (v_0). The graph was then modeled by the equation $\frac{Ax}{B+x}$, where A = k_{cat} and B = K_m.

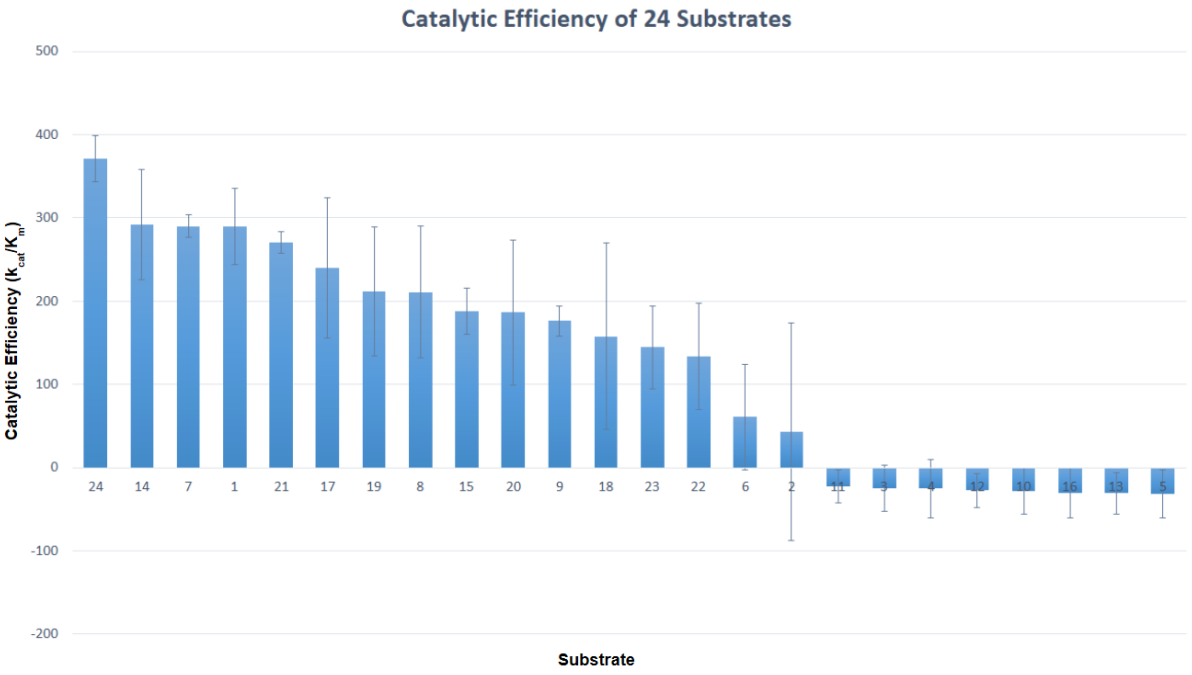

Figure 4. Catalytic efficiency of 24 substrates. The catalytic efficiency (k_{cat}/K_m) of 24 different substrates was tested to better characterize FoCdc14.

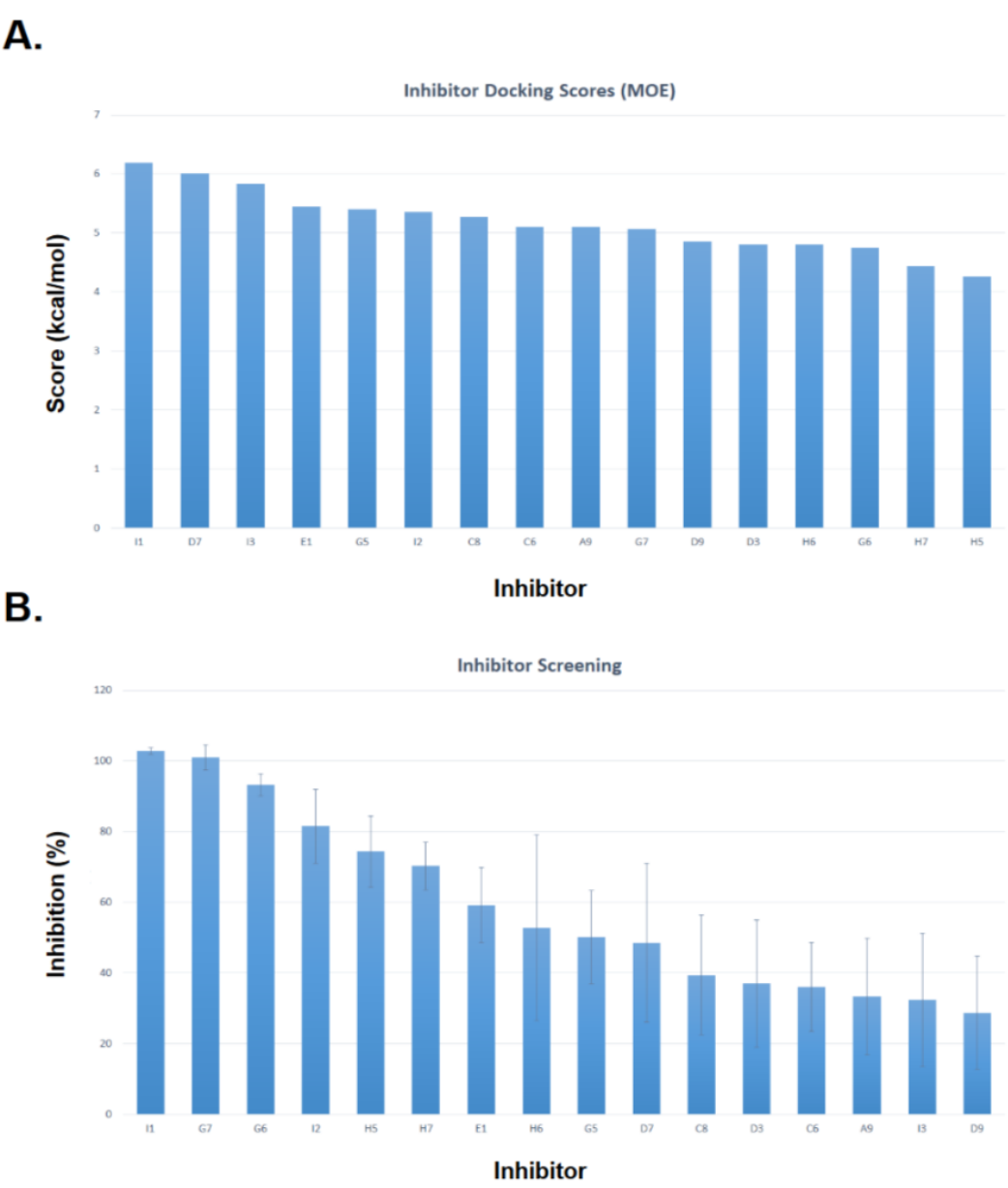

Figure 5. Inhibitor screening using computational and empirical techniques. (A) Inhibitors were modeled and docked in MOE and assigned a score. The more negative the score, the higher the affinity between the inhibitor and receptor. (B) Inhibitors were screened with FoCdc14 and pNPP. Percent inhibition was calculated based on a positive control of pure reaction between FoCdc14 and pNPP.

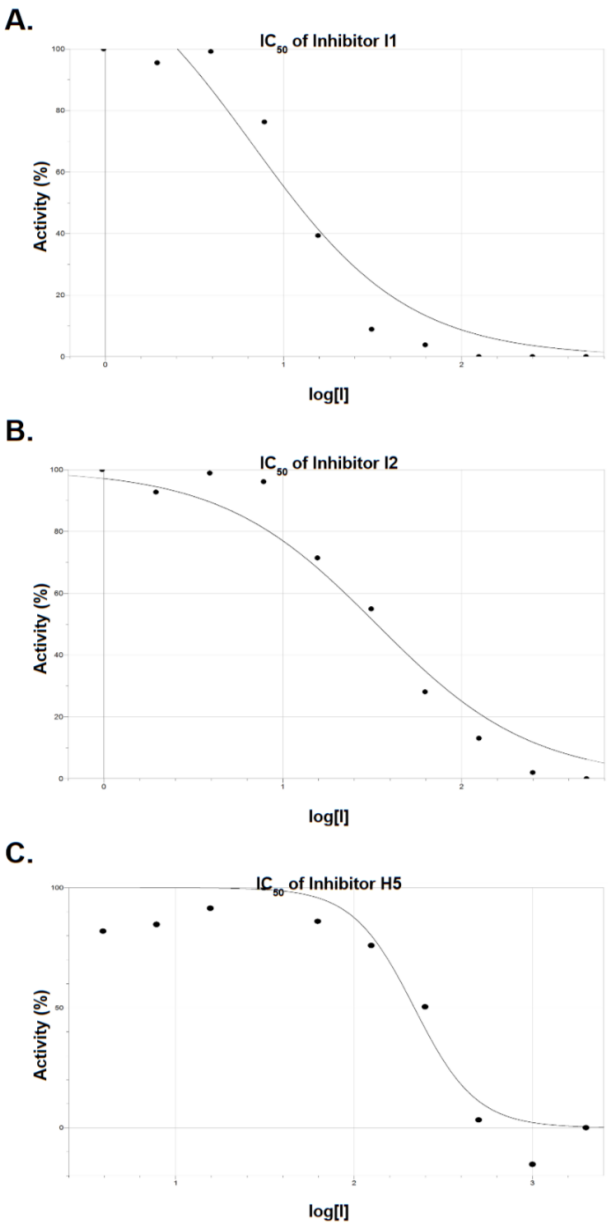

Figure 6. IC_{50} of selected inhibitors. The IC_{50} was found by curve fitting the equation $\frac{100}{1+10^{B(x-log(A))}}$ to a graph of percent activity vs. logarithm of inhibitor concentration (uM).

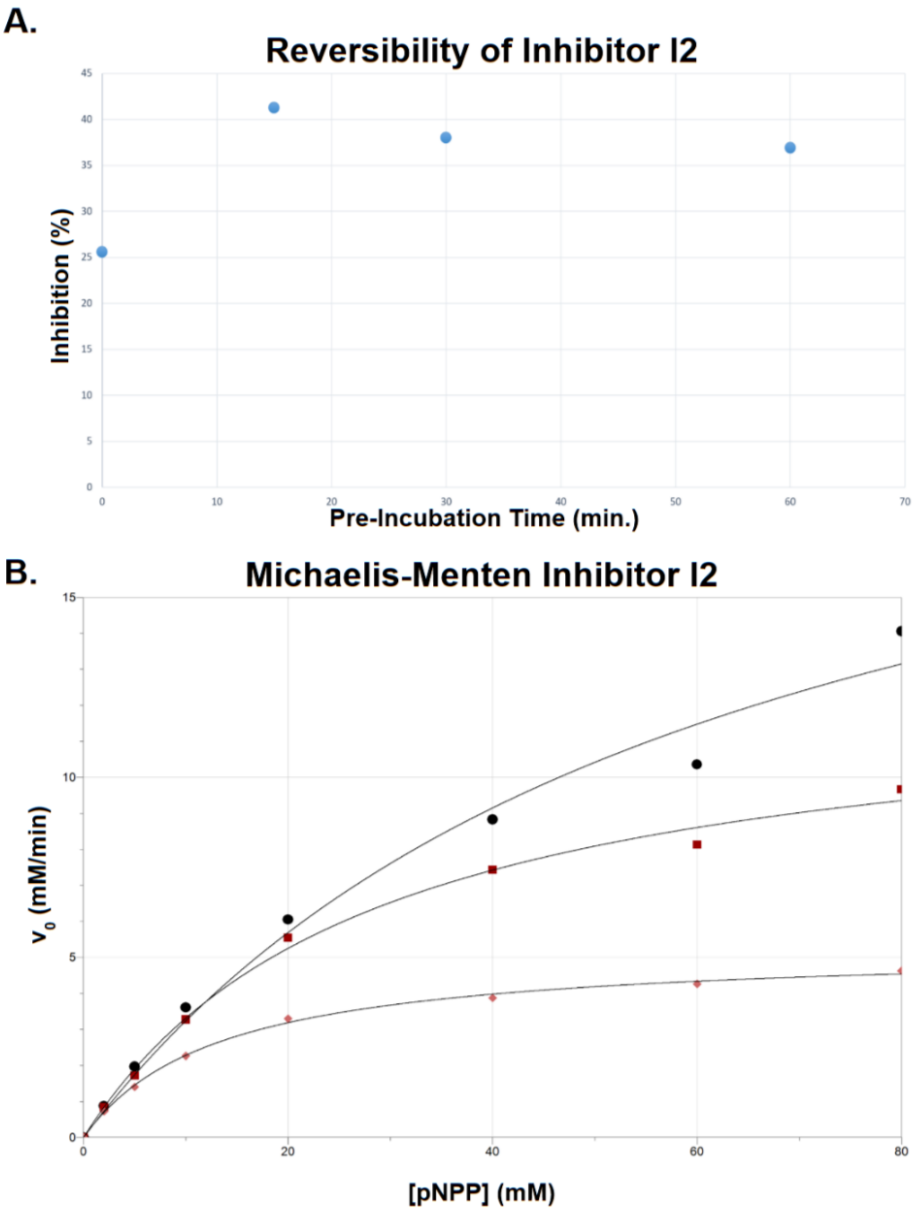

Figure 7. Inhibitor I2 is a reversible uncompetitive inhibitor in FoCdc14. (A) The pre-incubation time (the time before starting the reaction) has no correlation with the percent inhibition by I2. (B)The Michaelis-Menten curve fitting equation $\frac{Ax}{B+x}$ was fitted onto a graph of the concentration of substrate (pNPP) vs. initial velocity (v_0). ● Michaelis-Menten kinetics at 0 µM of inhibitor I2. ■ Michaelis-Menten kinetics at 25 µM of inhibitor I2. ◆ Michaelis-Menten kinetics at 50 µM of inhibitor I2.

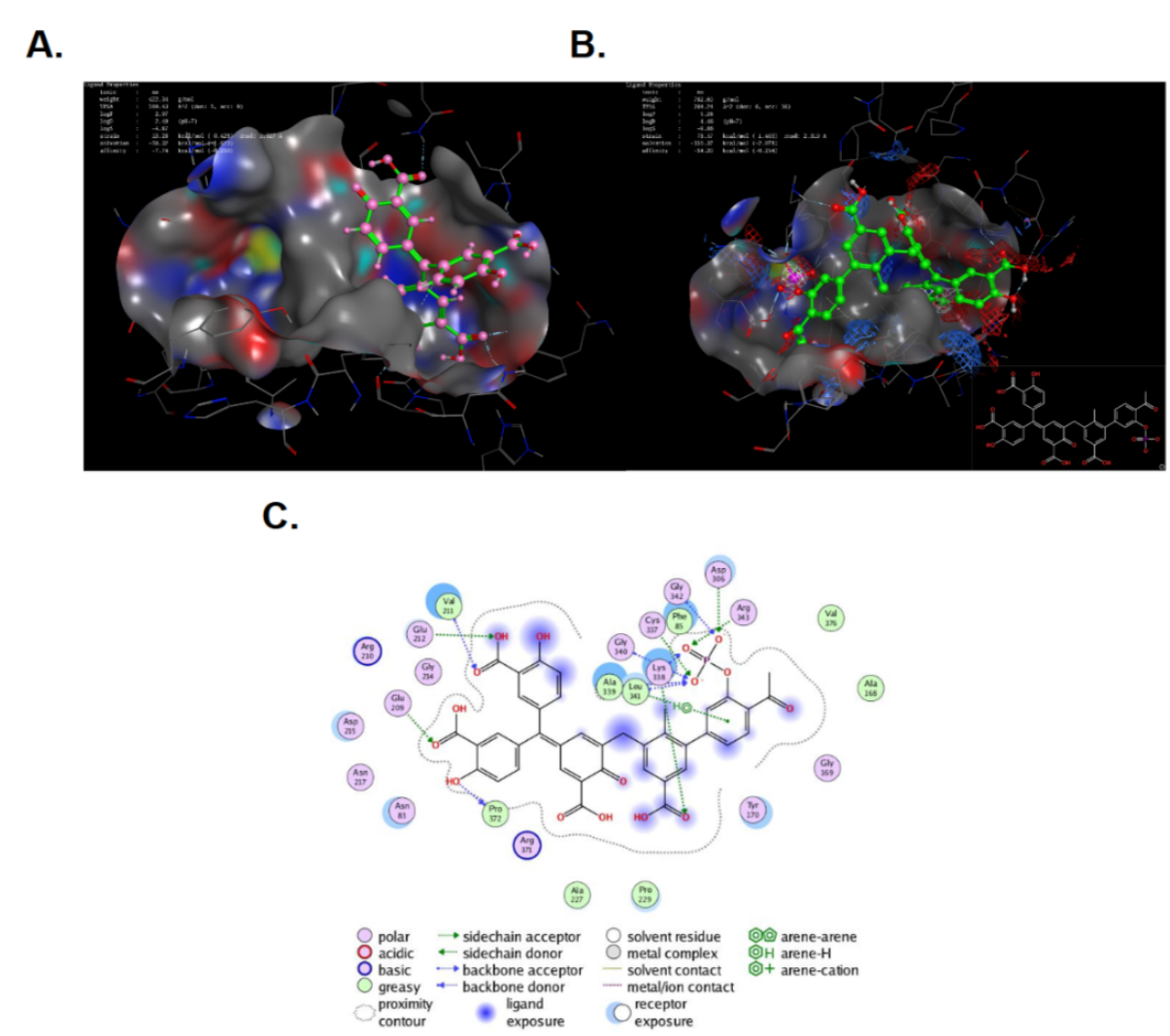

Figure 8. Optimization of Inhibitor I1 in FoCdc14. (A) The original inhibitor I1 (in green) is docked into the active site (shown by the surface map) of FoCdc14. (B) The 2D structure of the optimized inhibitor I1 is in the lower right corner. Inhibitor I1 is in green and surrounded by a surface map of the active site. Ligand properties are in the upper left corner. (C) The 2D interactions of the optimized I1 with the active site is shown.

Substrate 1	Substrate 2	Substrate 3	Substrate 4
HT{pS}PIKSIG	HT{pT}PIKSIG	HT{pY}PIKSIG	HT{pS}AIKSIG
Substrate 5	**Substrate 6**	**Substrate 7**	**Substrate 8**
HT{pS}PIASIG	HT{pS}PIRSIG	HT{pS}PIKKIG	HT{pS}PKKSIG
Substrate 9	**Substrate 10**	**Substrate 11**	**Substrate 12**
HT{pS}PIKSKG	HT{pS}PKASIG	HT{pS}PIAKIG	HT{pS}PIASKG
Substrate 13	**Substrate 14**	**Substrate 15**	**Substrate 16**
HT{pS}PIASIK	AT{pS}PIKSIG	HA{pS}PIKSIG	HT{pS}KIKSIG
Substrate 17	**Substrate 18**	**Substrate 19**	**Substrate 20**
HT{pS}PEKSIG	HT{pS}PIKEIG	HT{pS}PIKSEG	HT{pS}PIKSIE
Substrate 21	**Substrate 22**	**Substrate 23**	**Substrate 24**
HT{pS}PIKSIK	KT{pS}PIKSIG	HK{pS}PIKSIG	HT{pS}PIKKRG

Table 1. Tested substrate amino acid sequences. 24 substrates of varying sequences were tested for efficiency with FoCdc14. {pResidue} indicates a phosphoresidue.

A.

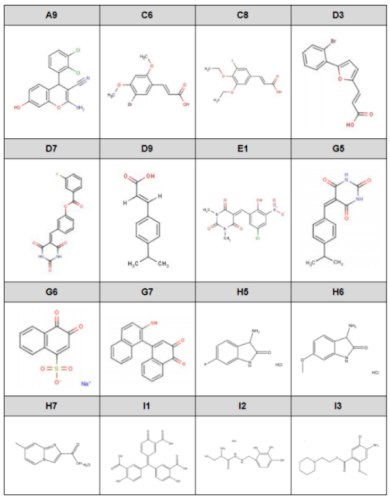

B.

Inhibitor	MOE Docking Score	% Inhibition
A9	-5.1067	33%
C6	-5.1077	36%
C8	-5.2730	39%
D3	-4.8059	37%
D7	-6.0166	49%
D9	-4.8509	29%
E1	-5.4493	59%
G5	-5.4009	50%
G6	-4.7516	93%
G7	-5.0746	101%
H5	-4.2644	74%
H6	-4.8053	53%
H7	-4.4354	70%
I1	-6.1867	103%
I2	-5.3613	82%
I3	-5.8265	32%

Table 2. Structure and result of screened inhibitors. (A) The structures of the 16 inhibitors that were screened as potential candidates for a fungicide are shown above. (B) Inhibitors were first docked into the molecular operating environment (MOE) and assigned a docking score. A more negative score (kcal/mol) indicates higher affinity to the active site. Assays were then run to determine the percent inhibition of each inhibitor.